Supplement of Atmos. Chem. Phys., 24, 5479–5494, 2024
https://doi.org/10.5194/acp-24-5479-2024-supplement

Atmospheric Chemistry and Physics
Open Access
EGU

Supplement of

Contribution of fluorescent primary biological aerosol particles to low-level Arctic cloud residuals

Gabriel Pereira Freitas et al.

Correspondence to: Paul Zieger (paul.zieger@aces.su.se)

Table S1. Data availability. Data availability (whole year, summer and winter seasons) of cloud events and sampled hours. These are subdivided for cloud events and sampled hours where the multiparameter bioaerosol spectrometer (MBS), temperature sensor (T), Cloudnet, isotope and Cloudnet+isotope data were available.

	Total	MBS	T	Cloudnet	Isotope	Cloudnet + isotope
Cloud events (all)	209	209	195	141	90	84
Sampled hours (all)	812	812	778	654	407	391
Cloud events (Summer)	156	156	142	93	42	41
Sampled hours (Summer)	612	612	578	470	241	241
Cloud events (Winter)	53	53	53	48	48	43
Sampled hours (Winter)	200	200	200	185	166	150

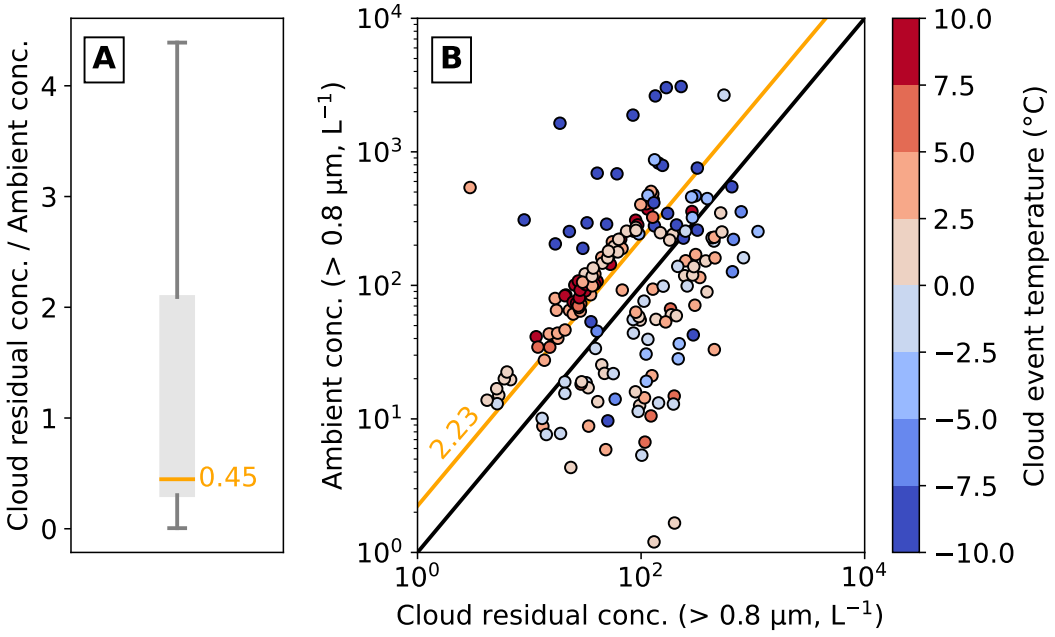

Figure S1. Comparison between ambient and cloud residual coarse-mode particles. A) A box plot of the ratio between cloud residual and ambient coarse-mode aerosol. Median is shown in orange (0.45). B) All cloud event cases are classified by temperature (color) and ambient/cloud residual coarse-mode aerosol. Black diagonal line is a 1x1 line, and orange line is the median ratio (2.23) between ambient aerosol and cloud residual.

1 Further case studies

1.1 Liquid cloud case

This is a case study that includes five clouds events (CE) that took place between 12 and 17 July 2020. The Cloudnet classification of these CE generally remained between cloud droplets (CD) and drizzle (DR, Figure S2-A), similar to that of a liquid cloud. Here, some of the CE, when visibility was low, did not completely coincide with the expected Cloudnet classification (e.g. Cloudnet classified the air above Ny-Ålesund as aerosol/clear sky, while the low visibility clearly indicated a presence of clouds at the observatory), exemplifying the differences between what was measured at the peak of the Zeppelin mountain and that above the Ny-Ålesund village. This discrepancy is due to the differences in wind pattern between the two sites (Pasquier et al., 2022). This was one limitation of this study, as sophisticated cloud probes were not available at such a comprehensive time frame as the methods used here.

The cloud persisted over northerly winds and low to medium wind speeds (Figure S2-B). Deuterium excess values were quite low (0–5 ‰) and followed quite closely the ambient air temperature that stayed always above 2.5 °C (Figure S2-C). During all 5 CE, the altitude at which the temperature reached - 15 °C hovered around 4800 meters and cloud top height was highly variable between 4 and 8 km (Figure S7). In fact, ice was present in the cloud at an altitude of 2000 meters. Given the high temperatures within the cloud at the height of the Zeppelin Observatory, not even the presence of high-temperature INP would give rise to ice formation within it. An indication that despite the presence of INP, meteorological conditions were not favorable for ice formation at the lower levels of the cloud, but ice formation was seen higher in the column at temperatures still above - 15 °C. However, it is not possible to clearly separate whether it is the result of primary ice nucleation or other glaciation mechanisms above that initiate secondary ice formation below.

Several fluorescent biological aerosol particles (fPBAP) were sampled by the MBS during these CE (Figure S2-D). Removing the 4th CE of this case study, in which the MBS was not fully operational, the MBS sampled 99 fPBAP, representing approximately 0.01% (or 1 in every 10^4 particles) of the total coarse-mode. Throughout the summer, fPBAP are ubiquitous at the Zeppelin Observatory (Pereira Freitas et al., 2023) and the results presented here show that they are present within clouds and possibly acted as cloud condensation nuclei. Under suitable conditions, they could contribute to glaciation and MPC formation.

1.2 Ice cloud case

This is a case study of 3 consecutive CE that took place during October 28th and 29th, 2020. These CE all had completely glaciated clouds (Figure S4-A). Across these events, significant cooling occurred (from -2.5 to -10°C) as the winds shifted to coming from the north and strengthened (10 ms^{-1}). Along with these changes, the d-excess shifted from relatively low values (0-5‰) to relatively high values (15-20‰), signaling a more transported source. During this cloud, the MBS detected 10 fPBAP (0.015% contribution to the coarse mode, Figure S4-D). The increase in deuterium excess during these events points to a shift to a more distant source of moisture in this winter case, and the temperature is low enough so that ice nucleation could have been started by INP of different activation temperatures along the cloud column. However, as mentioned above, the

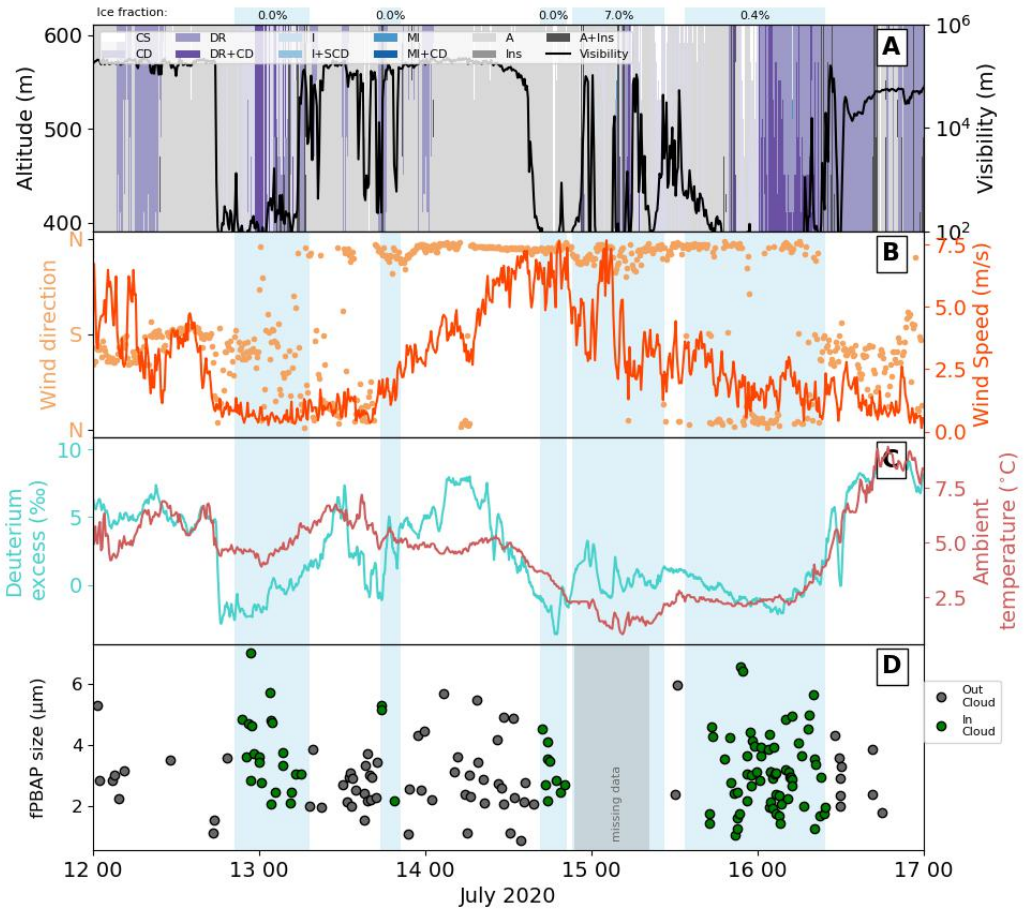

Figure S2. Example cloud events measured in July 2020. A) Cloudnet classification (at the height of Zeppelin observatory) and visibility (directly measured at Zeppelin observatory). Light blue boxes above and in the panels below indicate periods where counterflow virtual impactor (CVI) inlet sampling occurred along with the ice content of each CVI cloud event calculated using the Cloudnet data. B) Wind direction and speed at the Zeppelin observatory. C) Water vapor deuterium excess and ambient temperature. D) Fluorescent primary biological aerosol particles (fPBAP) measured by the multiparameter bioaerosol spectrometer (MBS) categorized by size. Out-cloud fPBAP are shown for context. Gray shaded area represents missing data from the MBS. Observations from panel B-D were taken at the Zeppelin observatory.

moisture and aerosol sources can, but not necessarily, be the same; thus, the deuterium excess values are only indicative. Given the meteorological conditions (Figure S5), little can be said about the influence of PBAP on this cloud. However, this shows that fPBAP are as evenly present in clouds as they are in the atmosphere throughout the year.

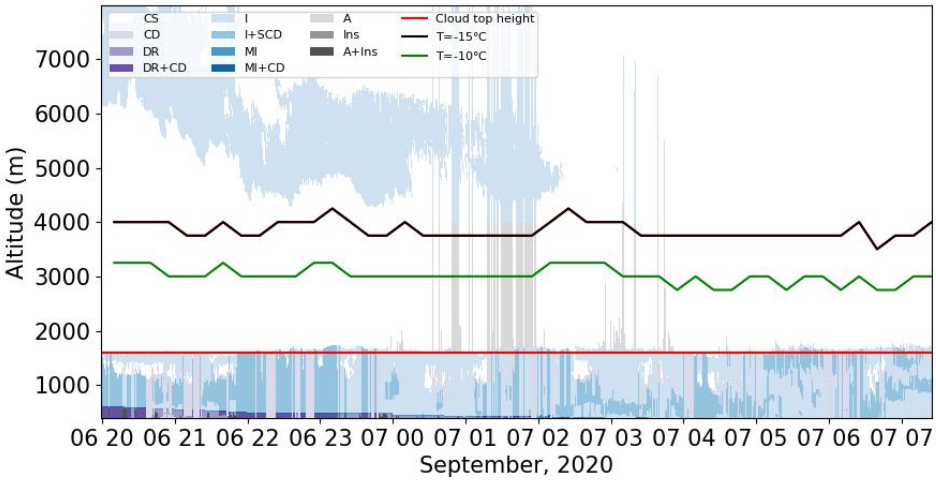

Figure S3. Full Cloudnet profile for mixed phase cloud case. Cloudnet profile along with assigned cloud top height and temperature curves for -15 °C and -10 °C.

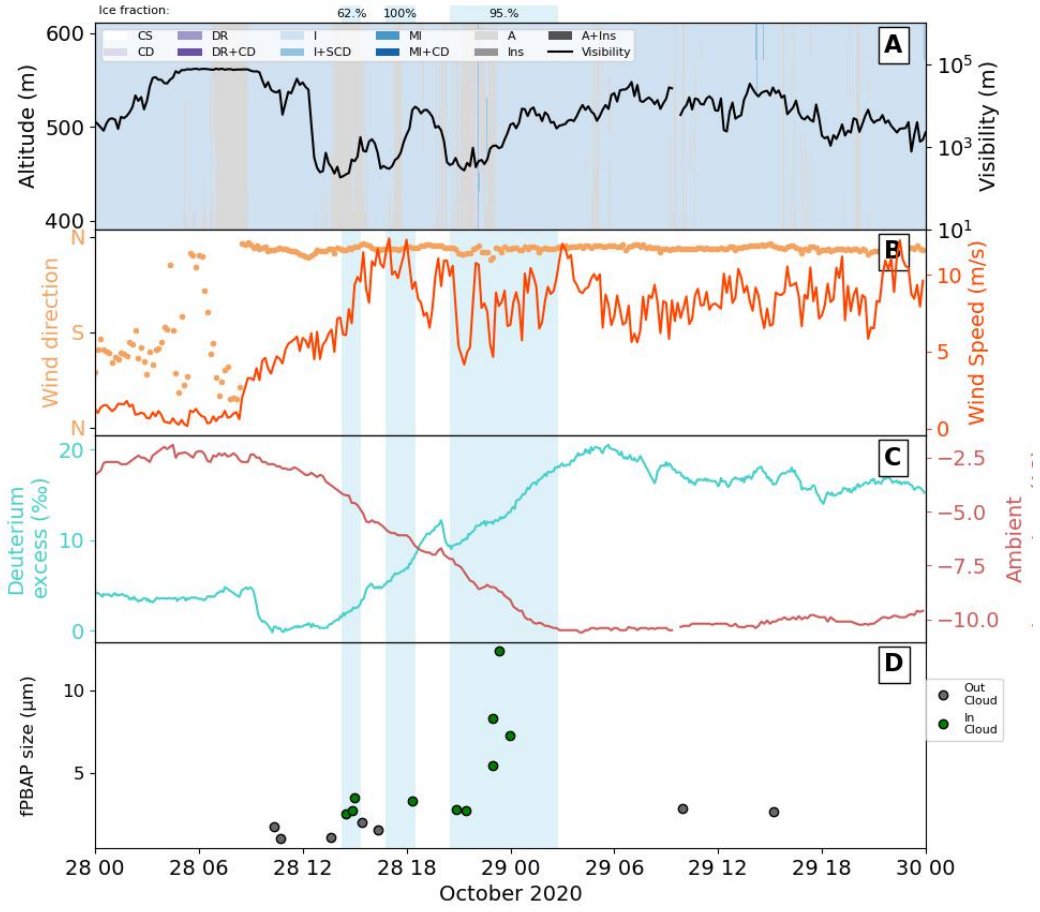

Figure S4. Example of an ice cloud event measured in October 2020. A) Cloudnet classification (at the height of Zeppelin observatory) and visibility (directly measured at Zeppelin observatory). Light blue boxes above and in the panels below indicate periods where counterflow virtual impactor (CVI) inlet sampling occurred along with the ice content of each CVI cloud event calculated using the Cloudnet data. B) Wind direction and speed at the Zeppelin observatory. C) Water vapor deuterium excess and ambient temperature. D) Fluorescent primary biological aerosol particles (fPBAP) measured by the multiparameter bioaerosol spectrometer (MBS) categorized by size. Out-cloud fPBAP are shown for context. Observations from panel b-d were taken at the Zeppelin observatory.

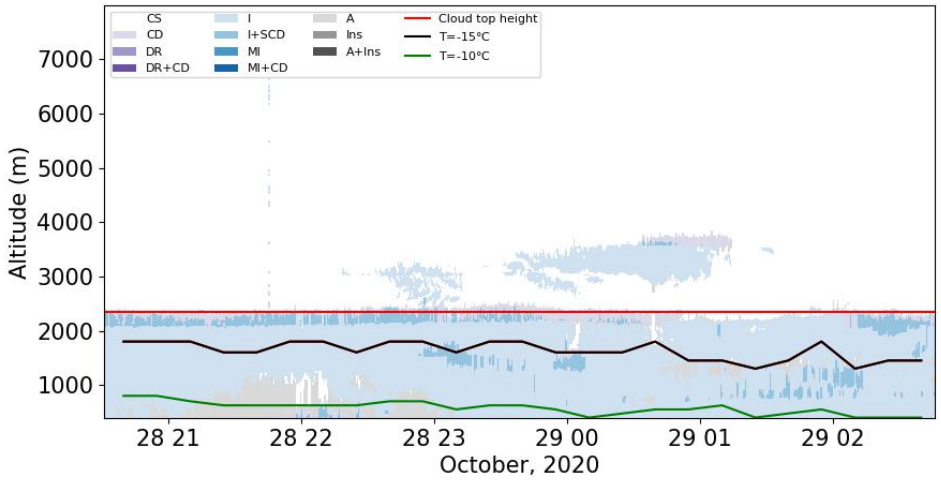

Figure S5. Full Cloudnet profile for ice cloud case. Cloudnet profile along with assigned cloud top height and temperature curves for -15 °C and -10 °C.

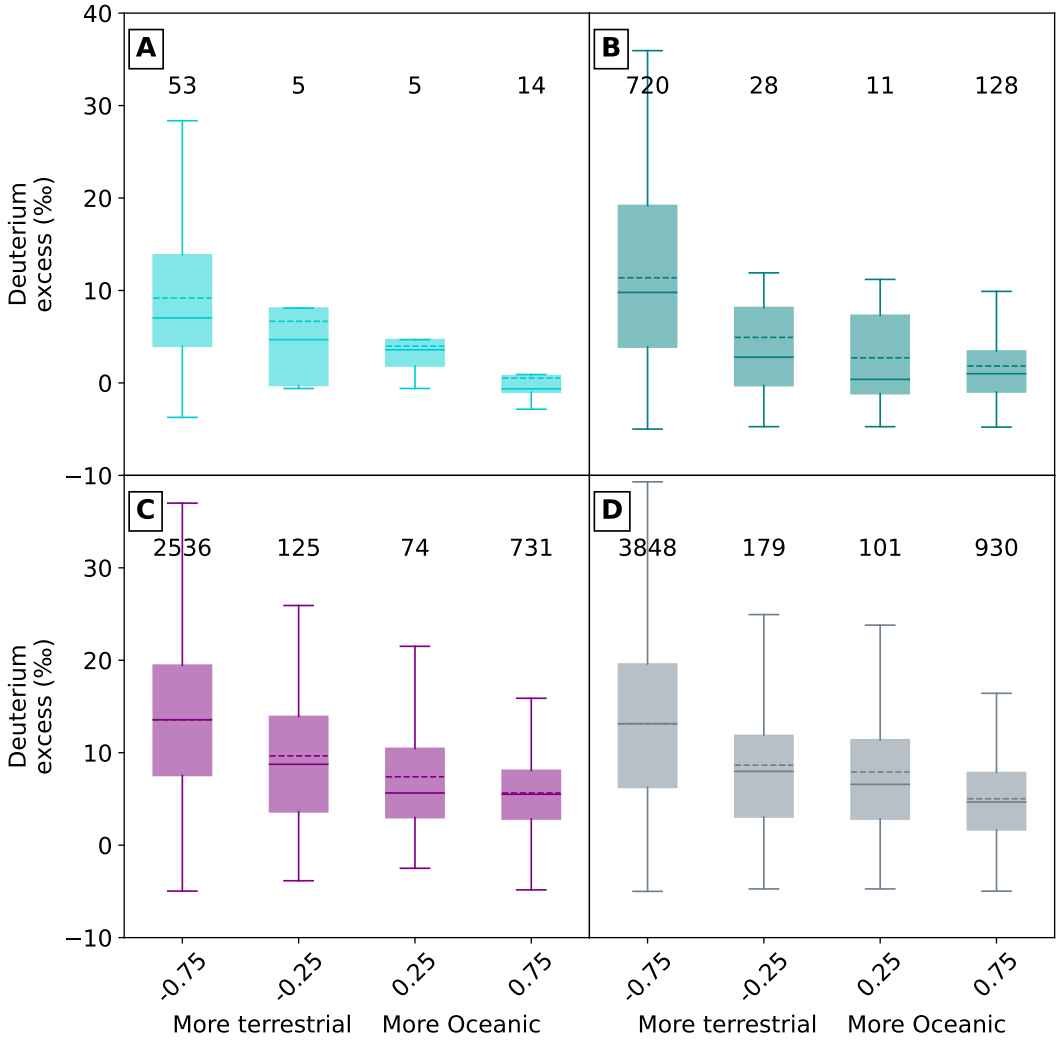

Figure S6. Deuterium excess (d-excess) as a function of trajectory type. Trajectory type (-1 fully terrestrial to 1 fully oceanic) and its deuterium excess for A) cloud cases, B) hours with visibility below 1000 meters, C) hours with visibility above 5000 meters and D) all data. Numbers represent number of points per box. The trajectory analysis and the parameter shown on the x-axis followed the approach, and is explained, by Zieger et al. (2015).

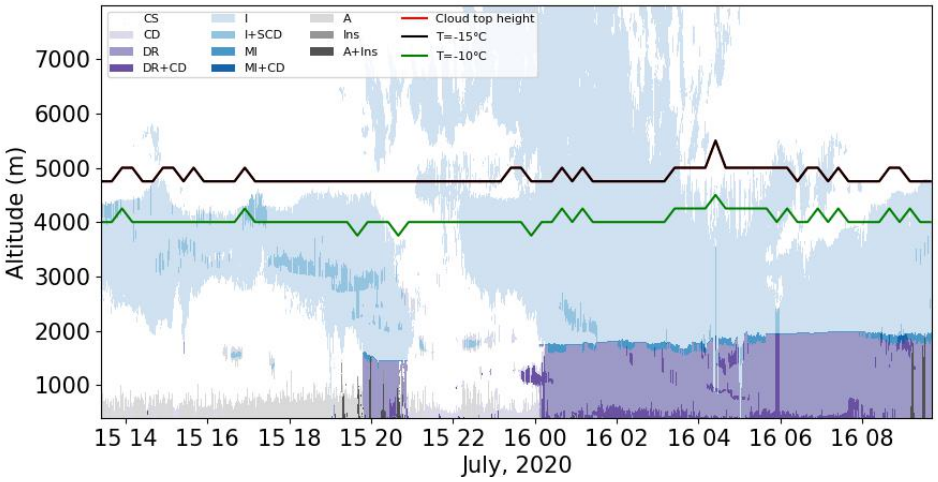

Figure S7. Full Cloudnet profile for liquid droplet cloud case. Cloudnet profile and temperature curves for -15 °C and -10 °C.

References

Pasquier, J. T., David, R. O., Freitas, G., Gierens, R., Gramlich, Y., Haslett, S., Li, G., Schäfer, B., Siegel, K., Wieder, J., Adachi, K., Belosi, F., Carlsen, T., Decesari, S., Ebell, K., Gilardoni, S., Gysel-Beer, M., Henneberger, J., Inoue, J., Kanji, Z. A., Koike, M., Kondo, Y., Krejci, R., Lohmann, U., Maturilli, M., Mazzolla, M., Modini, R., Mohr, C., Motos, G., Nenes, A., Nicosia, A., Ohata, S., Paglione, M., Park, S., Pileci, R. E., Ramelli, F., Rinaldi, M., Ritter, C., Sato, K., Storelvmo, T., Tobo, Y., Traversi, R., Viola, A., and Zieger, P.: The Ny-Ålesund Aerosol Cloud Experiment (NASCENT) Overview and First Results, Bulletin of the American Meteorological Society, 103, E2533–E2558, https://doi.org/10.1175/BAMS-D-21-0034.1, 2022.

Pereira Freitas, G., Adachi, K., Conen, F., Heslin-Rees, D., Krejci, R., Tobo, Y., Yttri, K. E., and Zieger, P.: Regionally sourced bioaerosols drive high-temperature ice nucleating particles in the Arctic, Nature Communications, 14, 5997, https://doi.org/10.1038/s41467-023-41696-7, 2023.

Zieger, P., Aalto, P. P., Aaltonen, V., Äijälä, M., Backman, J., Hong, J., Komppula, M., Krejci, R., Laborde, M., Lampilahti, J., De Leeuw, G., Pfüller, A., Rosati, B., Tesche, M., Tunved, P., Väänänen, R., and Petäjä, T.: Low hygroscopic scattering enhancement of boreal aerosol and the implications for a columnar optical closure study, Atmospheric Chemistry and Physics, 15, 7247–7267, https://doi.org/10.5194/acp-15-7247-2015, 2015.